Original Article
Food Science and Technology

ISSN 0101-2061 (Print)
ISSN 1678-457X (Online)

DOI: https://doi.org/10.5327/fst.04923

Polysaccharide from *Angelica sinensis* with medicinal and edible purposes ameliorated NAFLD by the bile acids mediated activation of FXR

Weiliang CHEN[1#], Li LUO[2,3#], Jun XIANG[4], Wu YUAN[5], Hanxiong DAN[1*], Kai-Ping WANG[6*]

Abstract

Liver and gut communicates with each other through metabolites and the gut-liver axis plays a crucial role in lipid metabolism. Enterohepatic bile acid circulation is an important constitution of gut-liver axis. Farnesoid X receptor (FXR), a bile acid mediated nuclear receptor, is promising therapeutic targets for the non-alcoholic fatty liver disease (NAFLD). More and more studies have confirmed the effects of *Angelica sinensis* polysaccharide (ASP) on liver protection and lipid regulation. However, little attention has been paid to the role of ASP on the gut-liver axis, which is crucial to clarify how ASP play a role in liver protection after oral administration. *In vivo* and *in vitro* models of NAFLD were established to examine the effect of ASP on hepatic fat accumulation. Our results showed that ASP could alleviate liver fat accumulation. However, the expression of FXR was not changed when ASP directly acting on hepatocytes, while ASP could change the expression of FXR in liver and intestine of mice after oral administration. In addition, our results showed that ASP could promote the excretion of bile acids, thereby increasing cholesterol metabolism. Our research provided a new concept for the mechanism of ASP regulating liver lipid metabolism and exerting liver protection.

Keywords: *Angelica sinensis* polysaccharide; non-alcoholic fatty liver disease; farnesoid X receptor.

Practical Application: This study will help to develop *Angelica sinensis* polysaccharide based functional foods for human consumption against non-alcoholic fatty liver disease.

1 Introduction

Nonalcoholic fatty liver diseases (NAFLD) is a multisystem disease and is considered the hepatic component of metabolic syndrome, which affects approximately 25% adult population worldwide (Powell et al., 2021). NAFLD can progress to nonalcoholic steatohepatitis (NASH) and other more progressive type of liver diseases. Furthermore, patients with NAFLD are at substantial risk for the development of type 2 diabetes mellitus, hypertension or coronary heart disease. This global liver disease will cause huge medical and economic burden (Younossi et al., 2016). Unfortunately, the pathogenesis of NAFLD is not fully clarified and no drug is approved for the treatment of NAFLD. It is mainly alleviated by lifestyle interventions, diet control, exercise and weight loss (Xu et al., 2020). However, pharmacological treatments and functional food intake are still very critical for NAFLD patients and worth more effort to explore.

Farnesoid X receptor (FXR), a nuclear receptor, is highly expressed in the liver and gut and known to exert tissue-specific effects in regulating bile acids (BAs) synthesis and transport (Chiang & Ferrell, 2022). Researches demonstrate that FXR plays a principle role in regulating lipid metabolism by inhibiting free fatty acid uptake and *de novo* lipogenesis, increasing fatty acid oxidation and exporting fat from hepatocytes (Chiang & Ferrell, 2020). BAs are nutrient sensors and metabolic regulators of FXR. BAs are converted from cholesterol in the liver and 75% BAs are synthesized by the classical pathway and catalyzed by the rate-limiting enzyme cholesterol 7α-hydroxylase (CYP7A1) (Chambers et al., 2019). The expression of CYP7A1 is regulated by various factors such as BAs, diet, circadian rhythms, hormones and cytokines. Its expression regulation mainly occurs at the transcriptional level and is controlled by nuclear receptors including FXR, LXR, PXR and PGC-1α (Beigneux et al., 2002). Dysregulation of bile acid homeostasis by high-fat diets is related to NAFLD.

Polysaccharides extracted from traditional Chinese medicines (TCM) showed great potential to alleviate pathological status of NAFLD by anti-inflammatory, regulating immunity, lowering blood glucose and lipids, and anti-oxidation (Chu et al., 2022; Li et al., 2022). The cholesterol-lowering property and bile acid metabolism regulation of polysaccharides are also well studied (Yang et al., 2022). ASP was extracted from the root of *Angelica sinensis (Oliv.) Diels*, a TCM used for gynecological and liver diseases. ASP could markedly improve metabolic dysfunction and oxidative stress in HFD-fed mice via the upregulation of PPARγ expression and the activation of adiponectin-SIRT1-AMPK signaling (Wang et al., 2016). It has been reported that only a small

Received 18 Jan., 2023
Accepted 28 Feb., 2023
[1] *Hubei Key Laboratory of Resources and Chemistry of Chinese Medicine, Hubei University of Chinese Medicine, Wuhan, China*
[2] *Department of Pharmacy, Union Hospital, Tongji Medical College, Huazhong University of Science and Technology, Wuhan, China*
[3] *Hubei Province Clinical Research Center for Precision Medicine for Critical Illness, Wuhan, China*
[4] *Hubei Institute of Measurement and Testing Technology, Wuhan, China*
[5] *Department of Biochemistry & Molecular Biology, Tongji Medical College, Huazhong University of Science & Technology, Wuhan, China*
[6] *Hubei Key Laboratory of Nature Medicinal Chemistry and Resource Evaluation, Tongji Medical College of Pharmacy, Huazhong University of Science and Technology, Wuhan, China*
*Corresponding author: wkpzcq@163.com; 1035988551@qq.com
[#] *Li Luo and Weiliang Chen share first authorship.*

amount of ASP could been absorbed by small intestine, most of the oral dosage was degraded into small molecular fragments in the large intestine or excreted (Wang et al., 2017). It aroused our great interest in whether the gut-liver axis plays a key role in ASP relieving NAFLD. In the present study, we established the *in vivo* NAFLD model to estimate the bile acid metabolism and FXR signaling regulation of ASP in liver and intestine. It will supply a better understanding of gut-liver axis theory of ASP in treatment of NAFLD. To the best of our knowledge, this is the first report to focus on ASP alleviating liver lipid metabolism via gut-liver axis related signal pathways. Clarifying the mechanism of ASP in preventing and treating NAFLD is of great significance to the development of ASP as a drug and functional food. *Angelica sinensis*, as a dual-use plant that can be used for both cooking and traditional Chinese medicine, will also receive more attention in daily diet.

2 Materials and methods

2.1 Chemicals and reagents

High-performance liquid chromatography grade formic acid and ammonium acetate, and BAs standards including cholic acid (CA), chendeoxycholic acid (CDCA), deoxycholic acid (DCA), lithocholic acid (LCA), glycocholic acid (GCA), taurocholic acid (TCA), glycochendeoxycholic acid (GCDCA), taurodeoxycholic acid (TDCA) and taurochendeoxycholic acid (TCDCA) were obtained from Sigma-Aldrich (St. Louis, Mo, United States) and the purity of the above reagents was higher than 98%.

2.2 Preparation of polysaccharide from Angelica sinensis

ASP were prepared according to the protocols previously described (Zhang et al., 2016). Briefly, the dry sliced roots of *Angelica sinensis* (Oliv.) Diels from Min County (Gansu Province, China) was treated with water extraction and alcohol precipitation to obtain the crude polysaccharide, which was further purified to remove proteins and small molecular impurities via repeated freeze dissolution and dialysis. Purified ASP was ultimately prepared through a gel filtration chromatograph with Sephadex G-50 and lyophilization.

2.3 Animals

Female SPF BALB/c mice at the age of 10 weeks were purchased from Beijing Vital River Laboratory. Mice were housed in a temperature-controlled environment (23 ± 2 °C) with a cycle of 12 h of light followed by 12 h of dark and free access to food and water. After 1 week of acclimatization, the mice were randomly divided into three groups (n = 8 per group): the control group (Con), in which mice were maintained on a standard chow diet; the high-fat diet group (HFD) and the treatment groups (ASP), in which mice were fed a high-fat diet for 12 weeks. The mice in the ASP groups were given orally with ASP which were dissolved in sterile saline (0.9% w/v) and filtered with a 0.22 μm filter membrane at a dosage of 160 mg/kg. Similarly, mice in the Con and HFD group were administered orally with sterile saline for four weeks. After being sacrificed, the serum, liver and intestine of the mice were collected and stored at -80 °C. Fecal samples were retained at -80 °C for later determination. All experimental animal experiments were conducted according to the Animal Care and Use Committee of Tongji Medical College (SYXK-2021-0057).

2.4 Cell culture

HepG2 cells were purchased from National Collection of Authenticated Cell Cultures (Shanghai, China). Cells were grown in DMEM (Gibco, C11995500BT) supplemented with 10% fetal bovine serum (Gibco), 1% penicillin-streptomycin (Biosharp, BL505A) in a 37 °C incubator with 5% CO_2. In order to induce NAFLD, 1×10^6 cells were seeded into six-well plates for 24 h and then stimulated with a 0.6 mM oleic acid/bovine serum albumin (OA/BSA) complex. After replicating the NAFLD model for 24 h, low-dose ASP (LASP, 100 μg/mL), medium-dose ASP (MASP, 250 μg/mL) and high-dose ASP (HASP, 500 μg/mL) in cultured medium were added to nourish the cells for 24 h.

2.5 Preparation of oleic acid/bovine serum albumin complex

First, 20 μL OA was added to 0.1 mol/L NaOH via 70 °C metal bathing for 30 min. Then, a 10% (w/v) BSA solution was prepared in PBS. Next, they were mixed and heated at 55 °C for 30 min to prepare a 10 mM OA stock solution. Finally, a 10 mM OA solution was diluted in DMEM to acquire a 0.6 mM OA solution.

2.6 H&E staining

Liver tissue samples were fixed with 4% paraformaldehyde and embedded in paraffin. Then, 5 μm thick sections were cut, and liver sections were stained with hematoxylin and eosin and examined under a microscope.

2.7 Western blot

Total protein was extracted using NP-40 lysis buffer (Beyotime Biotechnology, P0013F) containing a phosphatase and protease inhibitor cocktail (Thermo). After incubation on ice for 30 min, the mixtures were centrifuged at 12000 rpm for 15 min at 4 °C and quantified by a protein assay kit (Thermo). Samples containing the same amounts of protein were separated on 10% SDS-PAGE, followed by electrophoretic transfer to NC membrane, and immunoblotting with specific primary antibodies at a final dilution of 1:1000. Primary antibodies against farnesoid X receptor (FXR, 25055-1-AP), fatty acid synthase (FAS, 66591-1-lg), AMP-activated protein kinase (AMPK, 66536-1-lg) and sterol regulatory element-binding protein 1 (SREBP-1, 66875-1-lg) were purchased from Proteintech Co., Ltd (Wuhan, China). Antibody specific for FXR (1:200; sc-25309), SHP (1:200; sc-271511), CYP7A1 (1:200; sc-518007), FGFR4 (1:200; sc-136988) and FGF15 (1:200; sc-514647) were purchased from Santa Cruz Biotechnology (Santa Cruz, CA, USA). Antibody specific for tubulin and β-actin (1:1000; KTD101-CN) were purchased from Abbkine Scientific Co., Ltd (Wuhan, China). Blots were incubated with relative antibodies in 4 °C for overnight. Afterwards, goat anti-rabbit IgG or goat anti-mice IgG (Abbkine, 1:5000) was added for one hour in room temperature, and then the blots were developed with SuperSignal™ West Pico PLUS (Thermo,

34580). Quantification of the band intensity was performed using the ImageJ software (National Institutes of Health, USA).

2.8 The extraction of BAs in liver and feces

To obtain extraction of BAs in feces, 20 mg fecal sample was collected from each mice, adding 100 μL ultrapure water, acetonitrile and methanol successively and centrifuge for 15 min (12000 rpm, 4 °C) for three times. After each centrifugation, supernatant was absorbed and mixed with solvent for the next centrifugation. All the supernatants were mixed and added to glass vials for LC-MS analysis.

For liver BAs analysis, 50 mg liver tissue was excised to the tubes and washed in PBS. Then, adding 1.5 mL prechilled methanol/water (1:1) and homogenized the mixtures by Precellys beater. After that, centrifuging the mixtures for 10 min (14,000 g, 4 °C) and acquiring the supernatant. Dried in Vacuum concentrator, sediments were mixed with 1.6 mL dichloromethane/methanol (3:1). Finally, adding them to each glass vials for LC-MS analysis.

2.9 Metabolite analysis

Extract of livers and feces in mice were detected by HPLC-MS to quantify the content of BAs. The LC-MS portion of the platform was based on a HPLC (Ultimate 3000 UHPLC) system (Thermo Fisher Scientific) equipped with an Xbridge amide column (100 mm × 2.1 mm; inner diameter, 3.5 μm; Waters) and a Q Exactive mass spectrometer (Thermo Fisher Scientific). Liquid chromatography was performed as described below. The mobile phase A was 20 mM ammonium acetate and 15 mM ammonium hydroxide in water with 3% acetonitrile, pH = 9.0, and mobile phase B was acetonitrile. The linear gradient was as follows: 0 min, 85% B; 1.5 min, 85% B; 5.5 min, 30% B; 8 min, 30% B; 10 min, 85% B; and 12 min, 85% B. The flow rate was 0.2 mL·min^{-1}. Sample volumes of 5 μL were injected for LC-MS analysis. Data were quantified by integrating the area underneath the curve of each compound using the Xcalibur Qual browser (Thermo Fisher Scientific). Each metabolite's accurate mass ion and subsequent isotopic ions were extracted (EIC) using a 10 p.p.m. window.

2.10 Statistical analysis

Results are presented as the means ± SD of experiments performed in triplicate. The analysis was conducted using a statistical analysis software package (SPSS 26.0, Chicago, IL, USA). Significances of differences between mean values were determined using Student's t-test. Statistical significance was accepted for $P < 0.05$.

3 Result and discussion

3.1 Effect of ASP on HFD-induced hepatic lipid accumulation and steatosis

Body weight of mice was recorded during ASP treatment. Contrasted to the Con group, weight gain of HFD fed mice significantly increased. ASP treatment could inhibit the rising trend within a reasonable range (Figure 1B). Liver H&E staining showed that Con group mice preserved well cell structure. While HFD group mice showed obvious ballooning and clear indications of inflammation which were improved after ASP treatment (Figure 1C). Compared with the control group, the levels of total cholesterol (TC) and triglyceride (TG) in liver and serum of mice in HFD group were significantly increased. Our data showed that the increased TC and TG levels of HFD group were significantly revised by ASP (Figure 1D–G). These evidences indicated that ASP could alleviate hepatic steatosis in HFD-induced NAFLD mice.

3.2 ASP restored bile acid metabolism in NAFLD mice liver

Primary BAs, CA and CDCA, are synthesized in the liver and conjugated with either glycine or taurine. They are released into the duodenum after food consumption and recirculated to the liver from the terminal ileum (about 95%). Only a small part of BAs are either dehydroxylated or deconjugated by bacteria to form the secondary BAs: deoxycholic acid (DCA) or lithocholic acid (LCA) (Li & Dawson, 2019). CA, DCA and CDCA are the main bile acids cycling in gut-liver axis. High-fat diet induced lipid metabolism disorder and inhibited expression of CYP7A1 (Figure 2A–B). CYP7A1 is the key enzyme of liver cholesterol metabolism and the promoter of classic bile acid biosynthetic pathway in the liver (Chambers et al., 2019). Our data showed that ASP significantly revised expression of CYP7A1 in NAFLD mice liver. Subsequently, BAs were significantly decreased in the liver of HFD group ($P<0.01$) compared to Con group. Oral administration of ASP for 4 weeks, level of BAs was obviously improved (Figure 2C–I). Our work indicated that ASP could regulate BAs metabolism by promoting liver CYP7A1, and ultimately alleviate liver injury in HFD-induced NAFLD mice.

3.3 ASP alleviates the progress of NAFLD via activating liver FXR signaling in HFD mice

ASP obviously improved level of BAs, especially, CDCA and CA were almost recovered to the level of Con group (Figure 2C and 2E), which are more potent on FXR (Shin & Wang, 2019). BAs could protect against NAFLD progression through activating the FXR. It has been reported that FXR and FGF both participated to the mechanism of protection on steatosis (Schumacher & Guo, 2019). In liver, FXR-SHP plays a dominant role in decreasing TG level (Watanabe et al., 2004). Our previous research has clarified that ASP could down-regulate expression of hepatic CD36 and SREBP-1c to inhibit lipid uptake and lipogenesis (He et al., 2022). Researches showed that activated liver FXR down-regulated expression of CD36 and SREBP-1c. Oral administration of ASP revised the expression of liver CYP7A1 and increased bile acid synthesis. Furthermore, liver FXR was activated by the increased level of BAs, which is the only endogenous ligand of FXR (Jiang et al., 2021; Shin & Wang, 2019). In our study, ASP could restore liver FXR expression (Figure 3B) and activate downstream signals (Figure 3C–D) which were markedly decreased in HFD mice. These results further confirmed that ASP could alleviate the metabolism of BAs in the liver, thus causing the feedback regulation of FXR and the activation of FXR downstream protein in the liver.

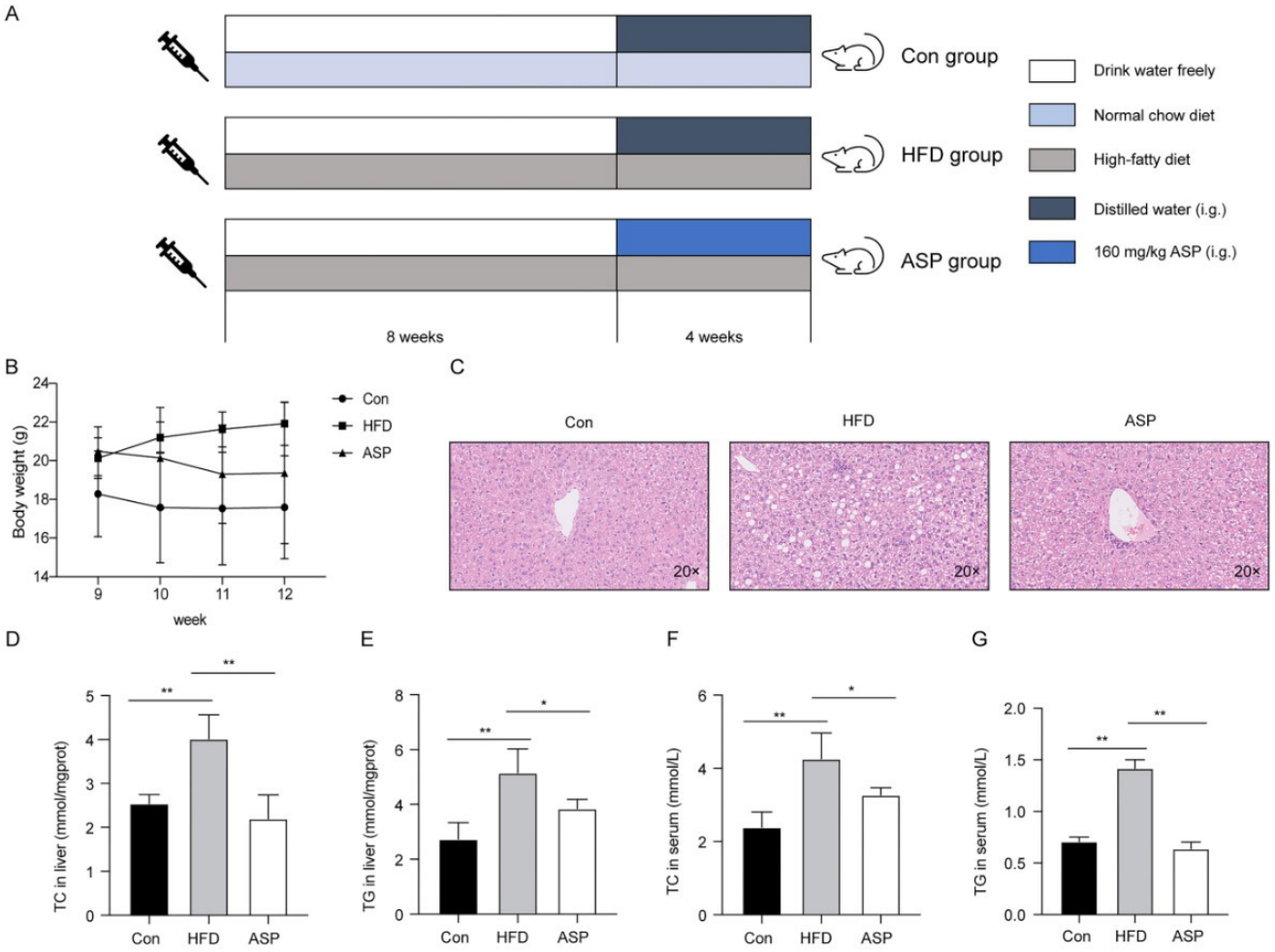

Figure 1. ASP decreased fat accumulation in mice liver. (A) Graphical protocol of animal experiment. (B) Changes of body weight in the period of ASP treatment. (C) Representative hematoxylin and eosin staining (20×) in the liver derived from each group. (D–E) Quantitation of liver TC and TG in mice. (F–G) Quantitation of serum TC and TG in mice.

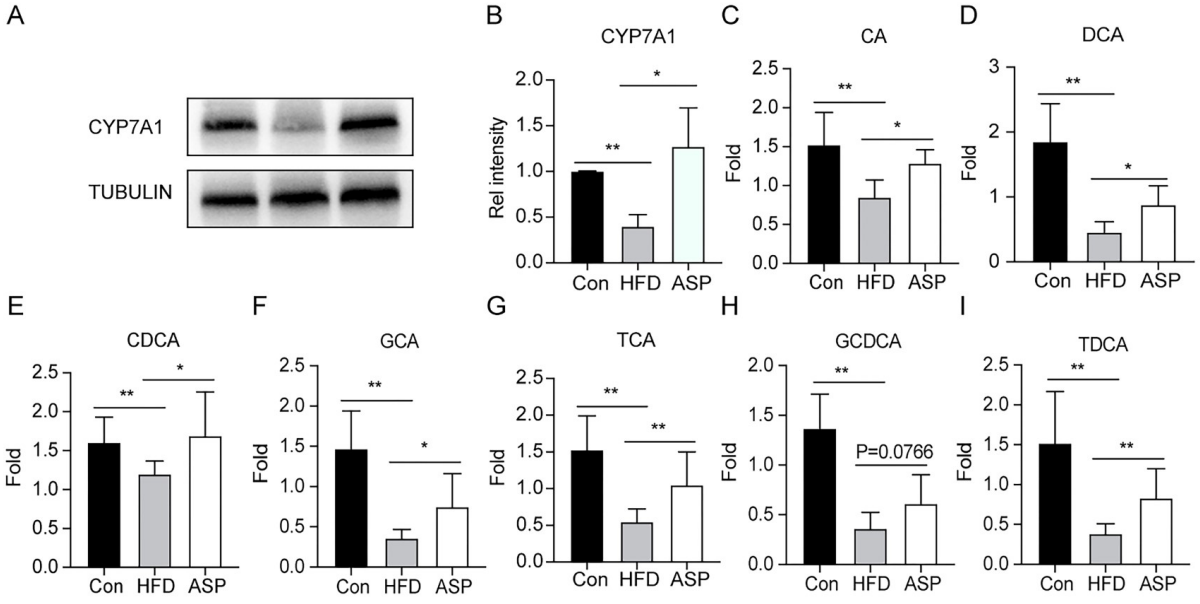

Figure 2. ASP increased bile acid in mice liver. (A) Western blotting was performed to determine hepatic protein levels of mice CYP7A1 and TUBULIN. (B) Densitometry analysis was performed to quantify the relative quantification of CYP7A1 band intensity divided by TUBULIN intensity. (C–I) Changes of CA, DCA, CDCA, GCA, TCA, GCDCA and TDCA in mice liver. Data are shown as mean ± SD. *P < 0.05, **P < 0.01.

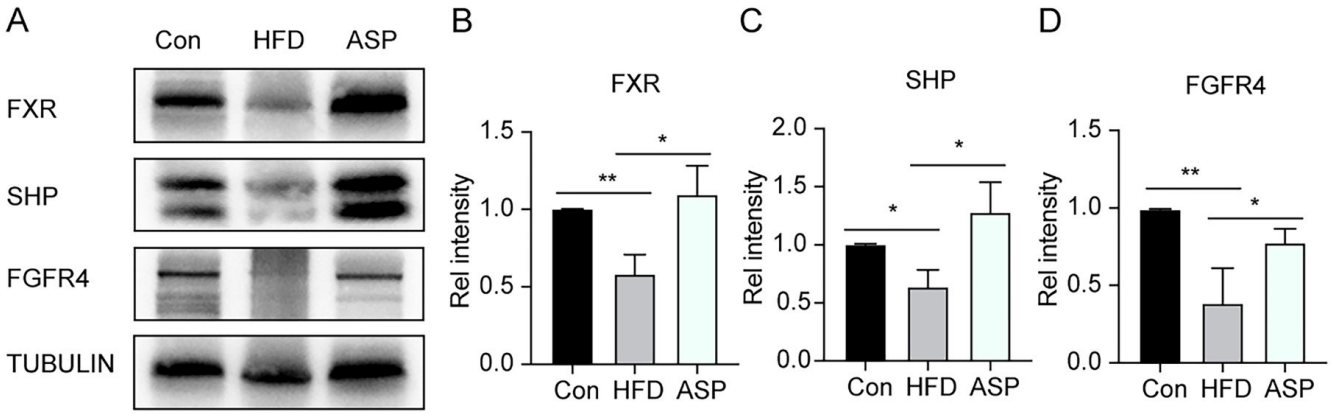

Figure 3. ASP alleviated NAFLD through FXR/SHP pathway in mice liver. (A) Western blotting was performed to determine hepatic protein levels of FXR, SHP, FGFR4 and TUBULIN. (B–D) Densitometry analysis was performed to quantify the relative quantification of FXR, SHP and FGFR4 band intensity divided by TUBULIN intensity. Data are shown as mean ± SD. *P < 0.05, **P < 0.01.

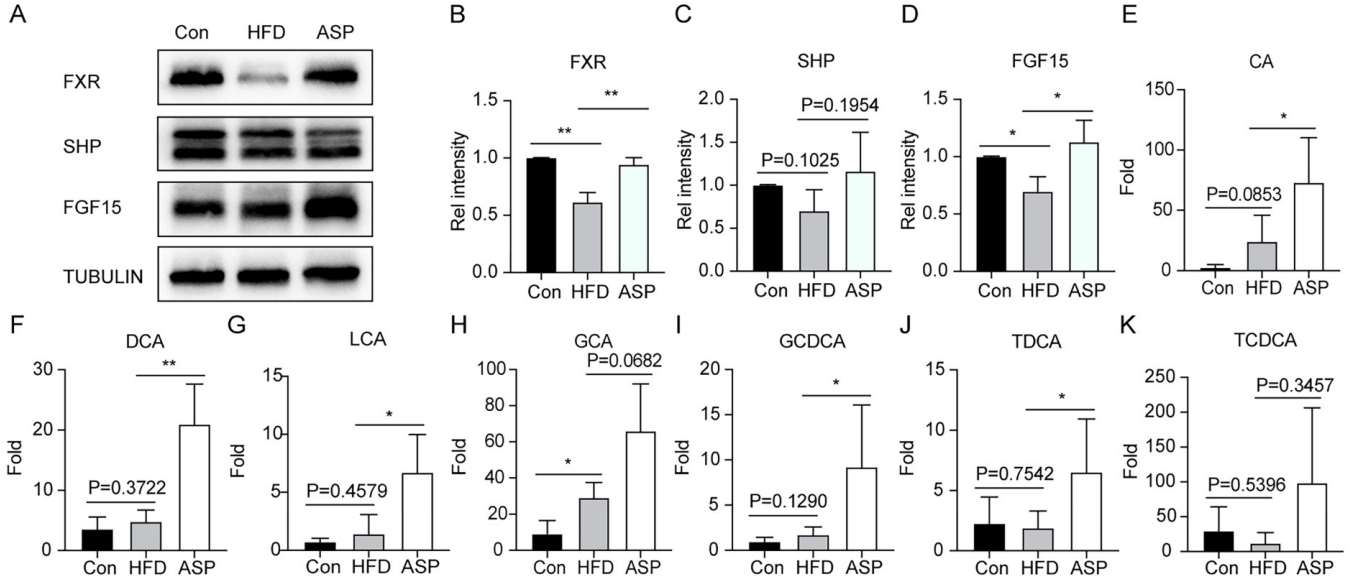

Figure 4. ASP alleviated NAFLD through FXR/FGF15 pathway in mice gut. (A) Western blotting was performed to determine enteric protein levels of mice FXR, SHP, FGF15 and TUBULIN. (B–D) Densitometry analysis was performed to quantify the relative quantification of FXR, SHP and FGF15 band intensity divided by TUBULIN intensity. (E–K) Changes of CA, DCA, LCA, GCA, GCDCA, TDCA and TCDCA in mice feces. Data are shown as mean ± SD. *P < 0.05, **P < 0.01.

3.4 ASP activated intestinal FXR signaling and increased excretion of fecal bile acid in HFD mice

Hepatic FXR plays an important role in prevention of hepatic lipid accumulation, whereas intestinal FXR controls lipid absorption. Emerging research suggested decreased intestinal lipid absorption required intestinal FXR-dependent BAs change (Jiang et al., 2015). The ASP treatment effectively reversed the down-regulation of intestinal FXR expression induced by high-fat diet (Figure 4A–B). Similarly, our data verified that ASP could also activate its downstream related proteins SHP and FGFR by increasing the expression of intestinal FXR (Figure 4A–D). The liver-gut axis is considered to play an important role in the occurrence and development of liver diseases, so the regulation of intestinal FXR and BAs is of great significance for the liver protection of NAFLD mice (Albillos, de Gottardi & Rescigno, 2020). The results of BAs in excreta showed that ASP could increase the excretion of BAs in HFD-induced NAFLD mice (Figure 4E–K). Studies have shown polysaccharides, such as β-glucan and pectin, could lead to an excess faecal BAs excretion and reduce serum cholesterol (Garcia-Diez et al., 1996; Marasca et al., 2020). Binding type experiment between BAs and ASP *in vitro* was carried out by LC-MS/MS in our study (Figure S1 - Supplementary Material). ASP showed good bile acid-binding capacity (Figure S2 - Supplementary Material). Therefore, ASP could increase the excretion of BAs from two aspects. First, the metabolism of BAs in the liver was increased, and the liver-gut circulation caused the increase of BAs in the intestine, thus increasing the excretion of BAs. Second, ASP, as

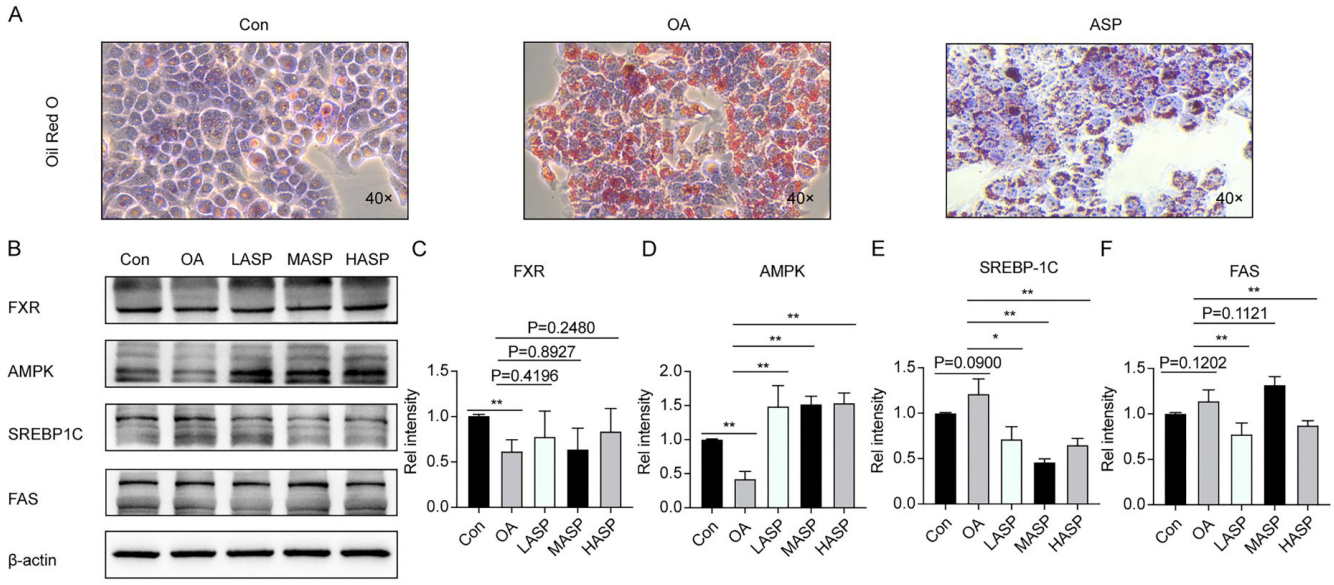

Figure 5. ASP regulated FXR and lipid metabolism in HepG2 cells. (A) The effects of ASP on lipid in NAFLD HepG2 cells by oil red O staining observation (40×). (B) The proteins expression of FXR, AMPK, SREBP1C, FAS and β-actin in HepG2 cells were measured by Western blot analysis. (C–F) Densitometry analysis was performed to quantify the relative quantification of FXR, AMPK, SREBP1C and FAS band intensity divided by β-actin intensity. Data are shown as mean ± SD. *P < 0.05, **P< 0.01.

a macromolecular polysaccharide, was difficult to be absorbed in the intestine, and directly combined with BAs in the intestine, thus increasing the intestinal excretion of BAs via forming a complex with BAs and excreting together. The results indicated that ASP could decrease lipid absorption by restoring intestinal FXR expression and reduce TC level in serum and liver via promoting BAs excretion.

3.5 ASP regulated lipid metabolism to ameliorate NAFLD in HepG2 cells

The *in vitro* NAFLD model was established to evaluate the effect of ASP on lipid metabolism in hepatocytes. MTT assay showed that ASP did not affect cell survival rate in the range of 0-1000 μg/mL. In our study, HepG2 cells were treated with OA and orange fat droplets were observed by oil red O staining after 48 h. After co-incubation with ASP, the orange fat droplets were greatly reduced in HepG2 cells (Figure 5A). It aroused our great interest in whether ASP could directly regulate the FXR of hepatocytes, and then regulated the metabolism of lipids in liver. Interestingly, ASP could not directly regulate the expression of FXR in hepatocytes (Figure 5B). This indicated that ASP did not play the role of lipid metabolism regulation by regulating FXR *in vivo* as its prototype, but might regulate FXR through its active fragment of intestinal metabolism or causing intestinal flora changes (Zhai et al., 2022). To confirm this hypothesis, we tested the influence of ASP on gut microbiota in HFD-induced NAFLD mice, and our results showed that ASP could significantly remodel the intestinal flora composition of NAFLD mice at the level of genus and species (Figure S3 - Supplementary Material).

Although ASP could not directly regulate the FXR expressions of hepatocytes, it could directly alleviate the accumulation of liver lipids, so important regulatory factor of lipid metabolism (AMPK) and metabolic enzymes associated with fat synthesis (SREBP-1c and FAS) were tested. Our results showed that ASP revised the down-regulation of AMPK induced by OA treatment and inhibited the expressions of SREBP-1c and FAS (Figure 5C–E). The results indicated that ASP could directly decrease lipid accumulation via FXR-independent pathway. ASP, as a macromolecular polysaccharide, was difficult to be absorbed as its prototype in the intestine, so, the FXR-independent pathway that ASP directly regulated the lipid metabolism of hepatocytes was not the main pathway for ASP exerting its liver protective effect by oral administration.

4 Conclusion

This study aimed to clarify mechanism of ASP treatment on HFD-induced NAFLD mice. Our results indicated that ASP could not directly regulate hepatic FXR *in vitro*, but it could improve liver lipid metabolism of NAFLD mice by regulating hepatic and intestinal FXR-related signal pathways after oral administration. This might be the result of the active fragment of ASP after intestinal metabolism or the regulation of intestinal flora. The mechanism of liver protection of polysaccharides after oral administration is very complex. This study provides a new insight on exploring the role of polysaccharides in liver protection through liver-gut axis after oral administration.

Conflict of interest

We declare no conflict of interests.

Funding

This research was financially supported by the National Natural Science Foundation of China (Grant No. 82204705 and 82074111).

Author contributions

Weiliang Chen: Writing – original draft, Data curation, Formal analysis. **Li Luo**: Conceptualization, Data curation, Funding acquisition. **Jun Xiang**: Data curation, Methodology. **Wu Yuan**: Formal analysis. **Hanxiong Dan:** Project administration, Writing – review & editing. **Kaiping Wang**: Supervision, Funding acquisition.

References

Albillos, A., Gottardi, A., & Rescigno, M. (2020). The gut-liver axis in liver disease: pathophysiological basis for therapy. *Journal of Hepatology*, 72(3), 558-577. http://dx.doi.org/10.1016/j.jhep.2019.10.003. PMid:31622696.

Beigneux, A., Hofmann, A. F., & Young, S. G. (2002). Human CYP7A1 deficiency: progress and enigmas. *The Journal of Clinical Investigation*, 110(1), 29-31. http://dx.doi.org/10.1172/JCI0216076. PMid:12093884.

Chambers, K. F., Day, P. E., Aboufarrag, H. T., & Kroon, P. A. (2019). Polyphenol effects on cholesterol metabolism via bile acid biosynthesis, CYP7A1: a review. *Nutrients*, 11(11), 2588. http://dx.doi.org/10.3390/nu11112588. PMid:31661763.

Chiang, J. Y. L., & Ferrell, J. M. (2020). Bile acid receptors FXR and TGR5 signaling in fatty liver diseases and therapy. *American Journal of Physiology. Gastrointestinal and Liver Physiology*, 318(3), G554-G573. http://dx.doi.org/10.1152/ajpgi.00223.2019. PMid:31984784.

Chiang, J. Y. L., & Ferrell, J. M. (2022). Discovery of farnesoid X receptor and its role in bile acid metabolism. *Molecular and Cellular Endocrinology*, 548, 111618. http://dx.doi.org/10.1016/j.mce.2022.111618. PMid:35283218.

Chu, X., Zhou, Y., Zhang, S., Liu, S., Li, G., & Xin, Y. (2022). Chaetomorpha linum polysaccharides alleviate NAFLD in mice by enhancing the PPARalpha/CPT-1/MCAD signaling. *Lipids in Health and Disease*, 21(1), 140. http://dx.doi.org/10.1186/s12944-022-01730-x. PMid:36529726.

Garcia-Diez, F., Garcia-Mediavilla, V., Bayon, J. E., & Gonzalez-Gallego, J. (1996). Pectin feeding influences fecal bile acid excretion, hepatic bile acid and cholesterol synthesis and serum cholesterol in rats. *The Journal of Nutrition*, 126(7), 1766-1771. PMid:8683337.

He, Z., Guo, T., Cui, Z., Xu, J., Wu, Z., Yang, X., Hu, H., Mei, H., Zhou, J., Zhang, Y., & Wang, K. (2022). New understanding of Angelica sinensis polysaccharide improving fatty liver: the dual inhibition of lipid synthesis and CD36-mediated lipid uptake and the regulation of alcohol metabolism. *International Journal of Biological Macromolecules*, 207, 813-825. http://dx.doi.org/10.1016/j.ijbiomac.2022.03.148. PMid:35358574.

Jiang, C., Xie, C., Li, F., Zhang, L., Nichols, R. G., Krausz, K. W., Cai, J., Qi, Y., Fang, Z. Z., Takahashi, S., Tanaka, N., Desai, D., Amin, S. G., Albert, I., Patterson, A. D., & Gonzalez, F. J. (2015). Intestinal farnesoid X receptor signaling promotes nonalcoholic fatty liver disease. *The Journal of Clinical Investigation*, 125(1), 386-402. http://dx.doi.org/10.1172/JCI76738. PMid:25500885.

Jiang, L., Zhang, H., Xiao, D., Wei, H., & Chen, Y. (2021). Farnesoid X receptor (FXR): structures and ligands. *Computational and Structural Biotechnology Journal*, 19, 2148-2159. http://dx.doi.org/10.1016/j.csbj.2021.04.029. PMid:33995909.

Li, J., & Dawson, P. A. (2019). Animal models to study bile acid metabolism. *Biochimica et Biophysica Acta. Molecular Basis of Disease*, 1865(5), 895-911. http://dx.doi.org/10.1016/j.bbadis.2018.05.011. PMid:29782919.

Li, X., Cui, W., Cui, Y., Song, X., Jia, L., & Zhang, J. (2022). Stropharia rugoso-annulata acetylated polysaccharides alleviate NAFLD via Nrf2/JNK1/AMPK signaling pathways. *International Journal of Biological Macromolecules*, 215, 560-570. http://dx.doi.org/10.1016/j.ijbiomac.2022.06.156. PMid:35772637.

Marasca, E., Boulos, S., & Nystrom, L. (2020). Bile acid-retention by native and modified oat and barley beta-glucan. *Carbohydrate Polymers*, 236, 116034. http://dx.doi.org/10.1016/j.carbpol.2020.116034. PMid:32172850.

Powell, E. E., Wong, V. W., & Rinella, M. (2021). Non-alcoholic fatty liver disease. *Lancet*, 397(10290), 2212-2224. http://dx.doi.org/10.1016/S0140-6736(20)32511-3. PMid:33894145.

Schumacher, J. D., & Guo, G. L. (2019). Pharmacologic modulation of bile acid-FXR-FGF15/FGF19 pathway for the treatment of nonalcoholic steatohepatitis. *Handbook of Experimental Pharmacology*, 256, 325-357. http://dx.doi.org/10.1007/164_2019_228. PMid:31201553.

Shin, D. J., & Wang, L. (2019). Bile acid-activated receptors: a review on fxr and other nuclear receptors. *Handbook of Experimental Pharmacology*, 256, 51-72. http://dx.doi.org/10.1007/164_2019_236. PMid:31230143.

Wang, K., Cao, P., Wang, H., Tang, Z., Wang, N., Wang, J., & Zhang, Y. (2016). Chronic administration of Angelica sinensis polysaccharide effectively improves fatty liver and glucose homeostasis in high-fat diet-fed mice. *Scientific Reports*, 6(1), 26229. http://dx.doi.org/10.1038/srep26229. PMid:27189109.

Wang, K., Cheng, F., Pan, X., Zhou, T., Liu, X., Zheng, Z., Luo, L., & Zhang, Y. (2017). Investigation of the transport and absorption of Angelica sinensis polysaccharide through gastrointestinal tract both in vitro and in vivo. *Drug Delivery*, 24(1), 1360-1371. http://dx.doi.org/10.1080/10717544.2017.1375576. PMid:28920748.

Watanabe, M., Houten, S. M., Wang, L., Moschetta, A., Mangelsdorf, D. J., Heyman, R. A., Moore, D. D., & Auwerx, J. (2004). Bile acids lower triglyceride levels via a pathway involving FXR, SHP, and SREBP-1c. *The Journal of Clinical Investigation*, 113(10), 1408-1418. http://dx.doi.org/10.1172/JCI21025. PMid:15146238.

Xu, Y., Guo, W., Zhang, C., Chen, F., Tan, H. Y., Li, S., Wang, N., & Feng, Y. (2020). Herbal medicine in the treatment of non-alcoholic fatty liver diseases-efficacy, action mechanism, and clinical application. *Frontiers in Pharmacology*, 11, 601. http://dx.doi.org/10.3389/fphar.2020.00601. PMid:32477116.

Yang, C., Huang, S., Lin, Z., Chen, H., Xu, C., Lin, Y., Sun, H., Huang, F., Lin, D., & Guo, F. (2022). Polysaccharides from Enteromorpha prolifera alleviate hypercholesterolemia via modulating the gut microbiota and bile acid metabolism. *Food & Function*, 13(23), 12194-12207. http://dx.doi.org/10.1039/D2FO02079C. PMid:36331041.

Younossi, Z. M., Koenig, A. B., Abdelatif, D., Fazel, Y., Henry, L., & Wymer, M. (2016). Global epidemiology of nonalcoholic fatty liver disease-Meta-analytic assessment of prevalence, incidence, and outcomes. *Hepatology (Baltimore, Md.)*, 64(1), 73-84. http://dx.doi.org/10.1002/hep.28431. PMid:26707365.

Zhai, Y., Zhou, W., Yan, X., Qiao, Y., Guan, L., Zhang, Z., Liu, H., Jiang, J., Liu, J., & Peng, L. (2022). Astragaloside IV ameliorates diet-induced hepatic steatosis in obese mice by inhibiting intestinal FXR via intestinal flora remodeling. *Phytomedicine*, 107, 154444. http://dx.doi.org/10.1016/j.phymed.2022.154444. PMid:36155217.

Zhang, Y., Zhou, T., Wang, H., Cui, Z., Cheng, F., & Wang, K. P. (2016). Structural characterization and in vitro antitumor activity of an acidic polysaccharide from Angelica sinensis (Oliv.) Diels. *Carbohydrate Polymers*, 147, 401-408. http://dx.doi.org/10.1016/j.carbpol.2016.04.002. PMid:27178946.

Supplementary Material

Supplementary material accompanies this paper.

Figure S1. The bile acid concentrations were determined by LC-MS/MS. (A) Chromatogram of internal standard IS and three bile acid standard mixed solution including cholic acid (CA), taurocholic acid (TCA) and glycylcholic acid (GCA); (B) Standard curve of CA; (C) Standard curve of TCA; (D) Standard curve of GCA.

Figure S2. Binding of ASP and bile acids (n=3). (A) Binding rate of ASP and bile acids; (B) Amount of bile acid binding per 100 mg ASP.

Figure S3. ASP treatment changed gut microbiota profile in HFD-induced NAFLD mice. (A) An unweighted unifrac cluster tree based on UPGMA showed similarity of intestinal microbiota in three groups. (B) Changes in the composition of the gut microbiota in different groups at the phylum level; stacked bar charts represent the relative abundance of major taxa. (C) Heatmap displayed different relative abundance among all genus and species. Different colors indicate different metabolite expressions (n = 7 per group).

This material is available as part of the online article from https://doi.org/10.5327/fst.04923